## Towards a novel method for liquefaction evaluation of silty sands

# Jun Yang i)

i) Professor, Department of Civil Engineering, The University of Hong Kong, Pokfulam, Hong Kong

#### **ABSTRACT**

Soil liquefaction is a subject of long-standing interest in earthquake geotechnical engineering. Although significant advances in liquefaction research have been achieved in the past decades, it remains an area of great difficulty and uncertainty, as evidenced by the extensive liquefaction-related damage in many recent earthquakes. Of particular concern is the widespread liquefaction observed in silty sand deposits, raising questions about the deficiencies of the current methods for liquefaction evaluation. This paper presents selected results of a long-term research aimed at developing a rational method for evaluating the liquefaction potential of both clean and silty sands. The method is based on a comprehensive experimental program comprising small-strain shear wave testing and large-strain undrained shear testing for a wide range of sand states and is built in the critical state framework. A remarkable feature of the method is the unified characterization of shear wave velocity for both clean and silty sands through a state parameter defined in a sound theoretical context. As shear wave velocity is a well-defined soil property and can be measured both in the field and in the laboratory, and since the state parameter has proven a useful state variable for characterizing soil behavior under both cyclic and monotonic loadings, the new method is attractive and promising in a wide range of geotechnical applications.

Keywords: liquefaction, silty sands, fines, shear wave velocity, critical state theory

### 1 INTRODUCTION

Soil liquefaction has been a subject of long-standing interest in geotechnical engineering. In the past decades, soil liquefaction has been investigated mainly in the context of earthquake loading (Seed 1979; Wang 1981; Ishihara 1993; Vaid et al. 2001; Youd et al. 2001; Idriss and Boulanger 2006), due to the significant liquefactionrelated damage observed during the Niigata and Alaska earthquakes in 1964 and many other earthquakes in the subsequent years. Some aspects of soil liquefaction have been well understood, many others, however, remain confusing, controversial or mysterious. The liquefaction phenomenon widely observed in undrained cyclic triaxial tests (Seed and Lee 1966) is characterized by repeated loss and regain of stiffness along with the development of excessive deformation. This behavior, known as cyclic mobility, may not be a true liquefaction phenomenon (Casagrande 1975; Castro 1975). Based on a comprehensive experimental program, Yang and his co-workers have shown that the undrained cyclic behavior of sand can be much more complicated than previously thought and can be categorized into five major modes: flow-type failure, cyclic mobility, plastic strain accumulation, limited flow followed by cyclic mobility, and limited flow followed by strain accumulation (Yang and Sze 2011a, 2011b; Sze and Yang 2014; Wei and Yang 2019a, 2019b). The question as to which pattern will occur depends on a number of inter-related factors, including packing density, effective confining stress, initial static shear stress level, cyclic load level, particle characteristics (e.g., size, shape, gradation and mineralogy), and soil fabric/structure.

Among the five deformation patterns, the flow-type failure is most critical and is characterized by abrupt, run-away deformation without any precautionary signal. This failure pattern is pertinent to sufficiently loose sand and in many ways is similar to the static or flow liquefaction phenomenon observed in monotonic triaxial tests (Yang 2002; Yamamuro and Lade 1997). Actually, there exists a good correspondence between the two (Yang and Sze 2011b), as shown in Fig. 1 in which the results from a monotonic test and a cyclic triaxial test on Toyoura sand at a similar post-consolidation state are plotted together. The flow liquefaction line, determined from the monotonic loading test, serves as a boundary in the stress space for the initiation of the flow-type failure. As for the cyclic mobility behavior, it is well linked with the dilative, strain-hardening response under the monotonic loading, as shown in Fig. 2. Essentially, cyclic mobility is a stable behavior rather than the metastable or unstable behavior of loose sand. It is worth emphasizing that flow liquefaction, triggered by either cyclic or monotonic loading, can produce the most catastrophic effects of all liquefaction-related phenomena and is thus a major concern in the design and construction of large earth structures such as tailings dams and artificial islands (Casagrande 1975; Jamiolkowski 2014). Caution is needed when using the conventional method to estimate the factor of safety of these earth structures since the method does not reflect the physics involved and can lead to unsafe prediction (Yang et al. 2022).

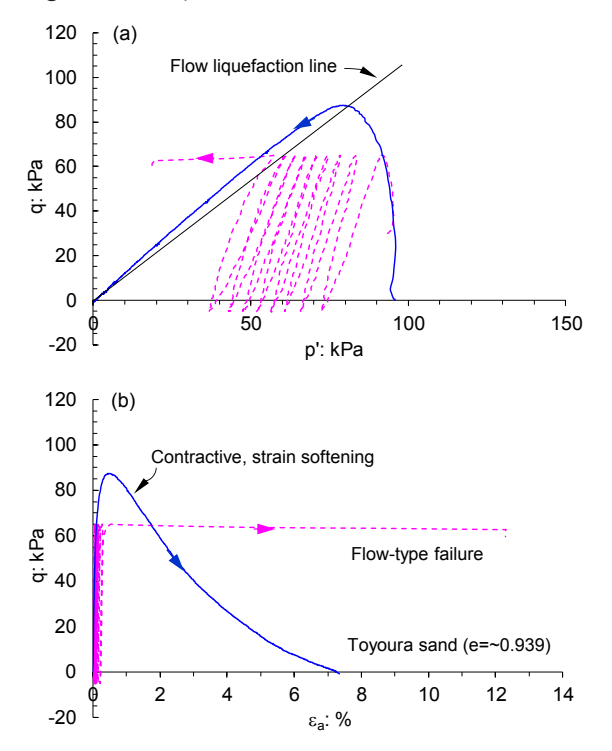


Fig. 1. Correspondence of flow liquefaction behavior under cyclic and monotonic loading.

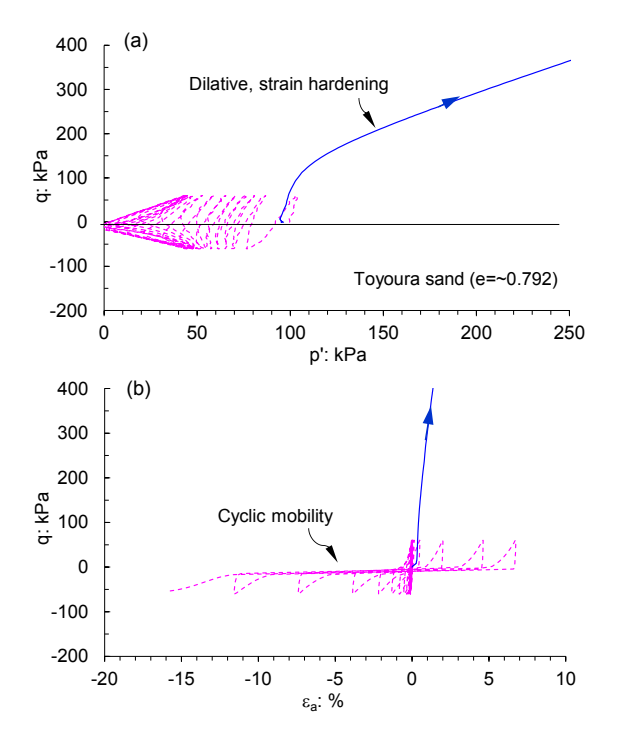


Fig. 2. Correspondence of cyclic mobility behavior and monotonic hardening behavior

Whether a sand is in a loose or dense state depends not only on its density (or void ratio) but also on the effective confining stress applied. There is now a general agreement that the behavior of a sand is more closely related to the proximity of its initial state to the critical state or steady state locus (Been and Jefferies 1985). which can be described by a state parameter  $(\psi)$  as shown in Fig. 3. If the initial state of a saturated sand lies above the critical state locus with a positive  $\psi$  value (state A in Fig. 3), it tends to contract when sheared undrained, accompanied by strain softening and a buildup of positive pore water pressure. If the initial state lies below the critical state locus with a negative w value (state D or B), it tends to undergo a net dilation, accompanied by strain hardening to a much higher strength. The initial state defined by the void ratio and mean effective stress with reference to the critical state locus is therefore a meaningful measure that can be used to quickly identify the potential for liquefaction.

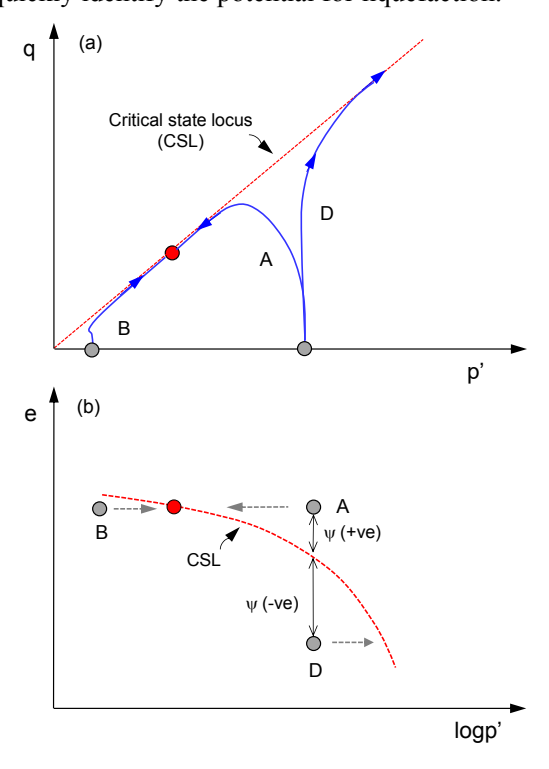


Fig. 3. Schematic illustration of state-dependent behavior of sand under undrained monotonic loading

Of particular interest is that the state parameter has been demonstrated to be a useful state variable for characterizing the cyclic resistance of sand under a range of initial states (Yang and Sze 2011a, 2011b; Wei and Yang 2023), as shown in Fig. 4 using the test data on Toyoura sand (TS), Fujian sand (FS) and Ottawa sand (OS), three uniform quartz sands. Here, CRR<sub>10</sub> is defined as the cyclic stress ratio causing failure in 10 stress cycles and is presented as a function of the state parameter prior to cyclic loading. Clearly, there is a good correlation between the two which can be described by an exponential function:

$$CRR_{10} = a \cdot \exp(-b \cdot \psi) \tag{1}$$

where a and b are fitting parameters. The central solid line in Fig. 4 is the best-fit trend line for test data on Toyoura sand (Yang and Sze 2011a), with a = 0.1653 and b = 6.161. The two dashed lines represent  $\pm 15\%$  deviations from the best-fit curve. Note that data points of Fujian sand and Ottawa sand also lie in the vicinity of the best-fit line, suggesting the rationale of the relationship.

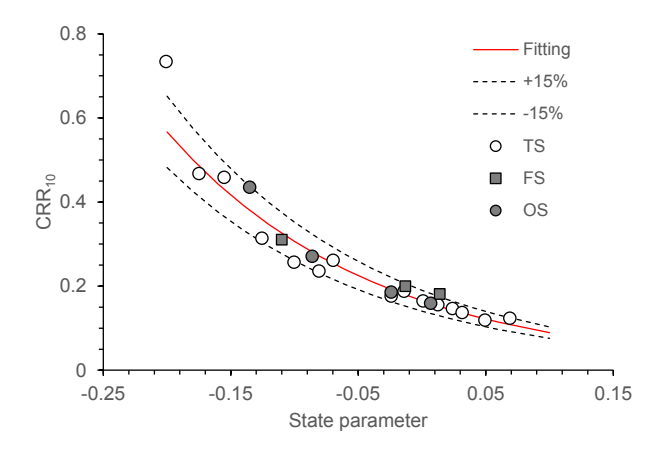


Fig. 4. Correlation between cyclic resistance and state parameter (data from Yang and Sze 2011; Wei and Yang 2023)

Along this line, we have attempted to develop a new method which allows unified evaluation of the state of both clean and silty sands and thereafter their potential liquefaction through shear wave velocity measurements in conjunction with the concept of state parameter. Theoretically, shear wave velocity is a fundamental soil property with clear physical meaning and is directly related to the elastic shear modulus of soil. Practically, modern technology has advanced such that shear wave velocity can be measured more conveniently and reliably both in the laboratory and in the field (Clayton 2011; Stokoe 2007). This paper describes the main aspects of this appealing method along with the validation and discussion. It is not the purpose of this paper to conduct a comprehensive literature review of the subject of soil liquefaction or liquefaction evaluation methods.

# 2 DIFFICULTY ASSOCIATED WITH SAND STATE EVALUATION

Using conventional methods to obtain undisturbed sand samples for laboratory testing remains a difficult problem in geotechnical engineering. As a consequence, significant efforts have been made to use field tests, particularly the cone penetration test (CPT), to estimate the in-situ state of sand (Baldi et al. 1982; Been et al. 1986). Central to the CPT-based method is an empirical correlation between relative density (or void ratio),

effective stress level and cone tip resistance, established mainly from laboratory chamber tests on clean uniform sands. Attempts have also been made to use shear wave velocity  $(V_s)$  to estimate the state of sand (Robertson et al. 1995). Similarly, the key to the  $V_s$ -based method is an empirical correlation linking void ratio, effective stress level and shear wave velocity, derived from laboratory measurements of shear wave velocity in clean sand samples. Often, natural sand deposits or fills are not clean, but contain a certain percentage of fines (referred to as silty sand in practice). Even within a single deposit of sand, the percentage of fines may vary appreciably. For example, the fill materials used in the construction of the artificial islands in the Beaufort Sea contained non-plastic fines at percentages varying from 0 to 12%. Application of the existing CPT- or  $V_s$ -based methods implicitly requires the assumption that the empirical correlations are not affected by the presence of fines. This assumption, however, is questionable.

It has been found that, for a given void ratio and confining stress, the shear wave velocity or the associated shear modulus of clean sand will change with the addition of fines (Yang and Liu 2016; Wichtmann et al. 2015). It has also been noted that the cone tip resistance can be affected by the presence of fines (Lunne et al. 1997; Mayne 2007), and this influence of fines may contribute to the considerable uncertainty associated with the correction factors for the interpretation of chamber testing data. In this connection, caution should be exercised when using the existing empirical methods to evaluate the state of silty sand deposits, since they could in some circumstances cause potentially catastrophic consequences.

### 3 IMPACT OF FINES ON LIQUEFACTION POTENTIAL OF SAND

There is an increasing amount of evidence showing that the presence of fines can alter the shear behavior of sand under either monotonic or cyclic loading conditions (Thevanayagam et al. 2000; Polito and Martin 2001; Murthy et al. 2007). However, as noted by Yang and Wei (2012), very diverse views exist as to whether the effect of fines is negative or beneficial for liquefaction resistance. The problem is complex due mainly to the fact that sand-fines mixtures are granular materials in nature. The characteristics of both fine and coarse particles, such as shape, size and plasticity, can affect the packing pattern and interactions of the particles and, hence, their mechanical behavior (Yang and Wei 2012; Wei and Yang 2014). Also, it is important to choose a proper density index as the basis for comparison of the responses of clean and silty sands (Yang et al. 2015; Wei and Yang, 2019b).

Fig. 5 shows an excellent example that the addition of non-plastic fines (crushed silica) to Toyoura sand can lead to a notable increase in strain softening compared with the base sand on its own at a similar (global) void

ratio. Under otherwise similar conditions, the specimen at fines content (FC) of 15% (denoted as TSS15) underwent complete liquefaction when subjected to undrained monotonic shear, whereas the clean sand specimen (TS) exhibited a strong dilative response with much high strength at large strains. Experimental evidence for the impact of fines on cyclic stress-strain behavior, pore water pressure generation and liquefaction resistance of two different sands is shown in Figs. 6 and 7.

In Fig. 6, the response of a loose Toyoura sand specimen under undrained cyclic loading is compared with that of a loose specimen of the same sand mixed with 10% fines (TSS10) under similar testing conditions. While both specimens exhibited the flow-type behavior, the TSS10 specimen quickly failed in less than 10 cycles of loading, but the TS specimen did not fail until ~78 loading cycles. Fig. 7 compares a medium-dense Ottawa sand specimen (OS) with a specimen of the same sand mixed with 20% non-plastic fines (OSS20) and consolidated to approximately the same state. Interestingly, the presence of fines can turn the response from cyclic mobility to the flow type although the cyclic load level applied to the OSS20 specimen is much less.

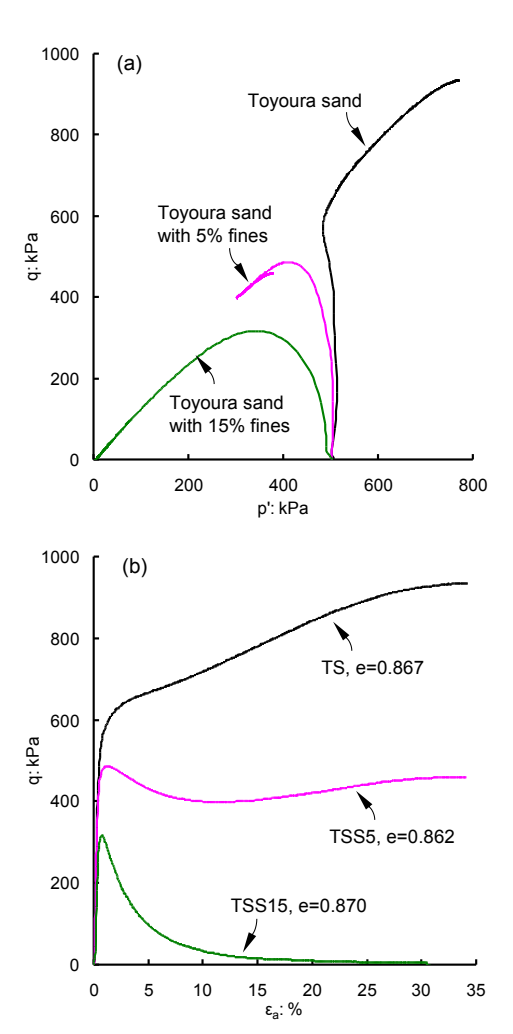


Fig. 5. Effect of fines on undrained behavior of sand under monotonic loading (data from Yang and Wei 2012)

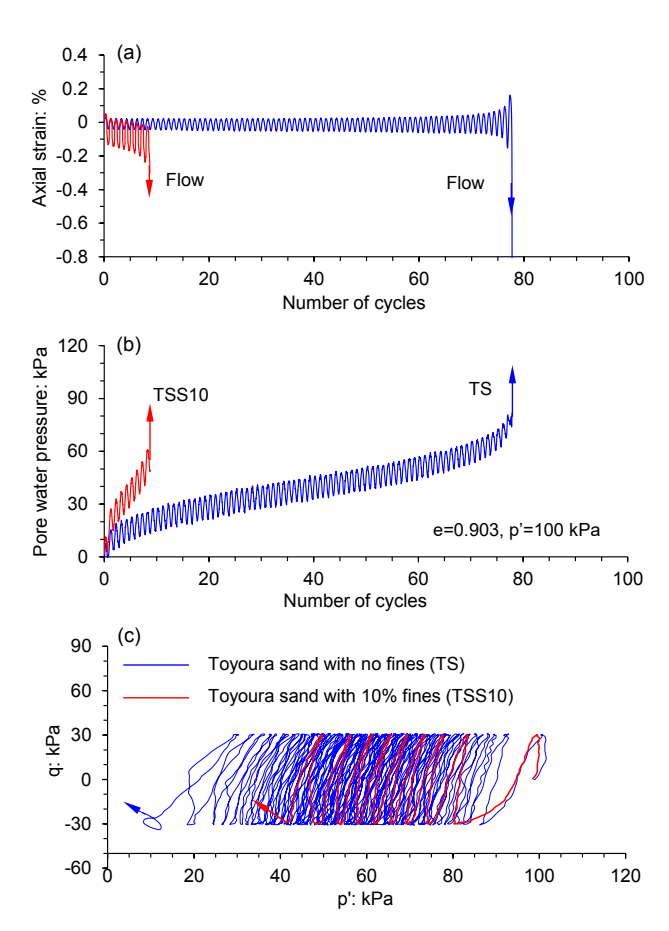


Fig. 6. Effect of fines on undrained cyclic behavior of Toyoura sand

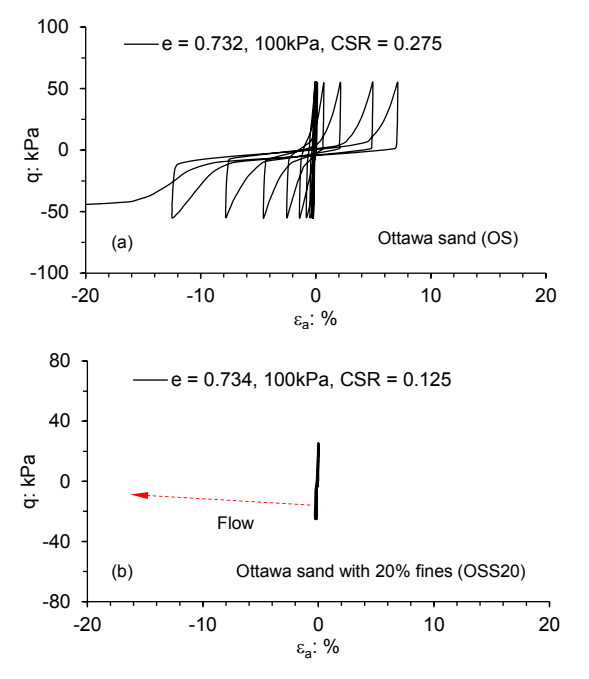


Fig. 7. Effect of fines on undrained cyclic behavior of Ottawa sand

For either monotonic or cyclic loading tests, the effect of non-plastic fines is always an increase in liquefaction potential or a decrease in liquefaction resistance if the post-consolidation void ratio is used

consistently as the comparison basis. Yang et al. (2015) have elaborated that the conventional (global) void ratio is a more rational state variable compared with such others as relative density and skeleton void ratio for sand-fines mixtures. Also, it is worth noting that the fines contents concerned here are less than the so-called threshold value, typically ~30%, such that all the sand-fines mixtures are considered as sand dominant.

# 4 SHEAR WAVE VELOCITY OF SAND AFFECTED BY FINES

A systematic investigation of the state-dependent shear wave velocity in saturated sand samples with different percentages of fines has been carried out using a resonant column apparatus embedded with piezo-electric elements (see Fig. 8). As an example, Fig. 9 shows shear wave signals recorded in four specimens of Toyoura sand mixed with different percentages of fines (TS, TSS10, TSS20, TSS30). All the four specimens were consolidated to a similar state, and the excitation frequency was set as 10 kHz. It is evident that the presence of a small quantity of fines can lead to a delay in the arrival time of shear waves and, thereafter, a reduction of shear wave velocity. More detailed information about the method of signal interpretation can be found in Yang and Gu (2013) and Gu et al. (2015).

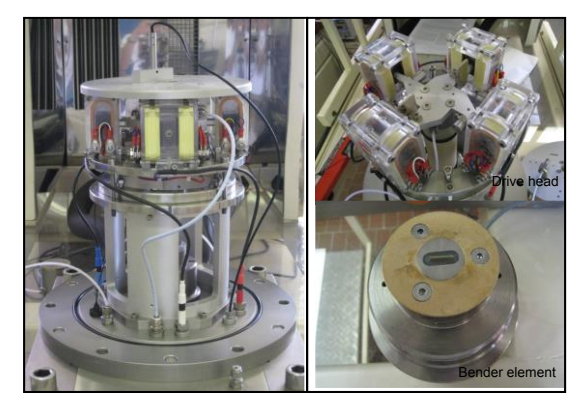


Fig. 8. Resonant column apparatus with bender elements embedded

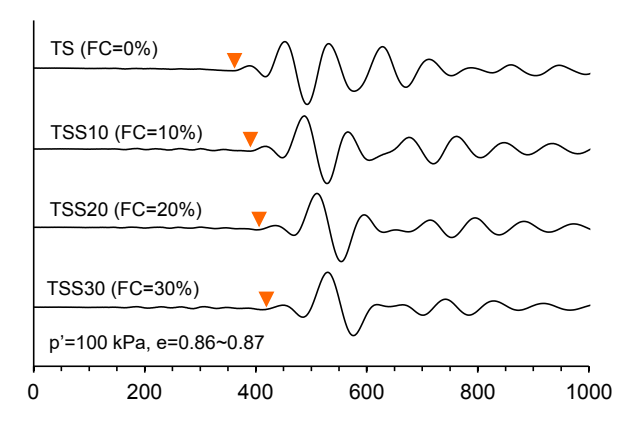


Fig. 9. Shear wave signals at excitation frequency of 10 kHz in saturated sand specimens with different percentages of fines

# 4.1 Void Ratio-based characterization of shear wave velocity

Measured  $V_s$  values for saturated sand specimens with different percentages of fines (TS, TSS5, TSS10 and TSS20) are plotted as a function of void ratio for two stress levels in Fig. 10. Clearly, in addition to the void ratio,  $V_s$  is also dependent on confining stress and fines content. The state dependence of  $V_s$  is often described using the following relationship (Hardin and Richart 1963; Robertson et al. 1995):

$$V_{s} = (b_{1} - b_{2}e) \left(\frac{p'}{p_{a}}\right)^{1/4} \tag{2}$$

where  $p_a$  is a reference pressure, typically taken as the atmospheric pressure. Notice that parameters  $b_1$  and  $b_2$  will vary with fines content.

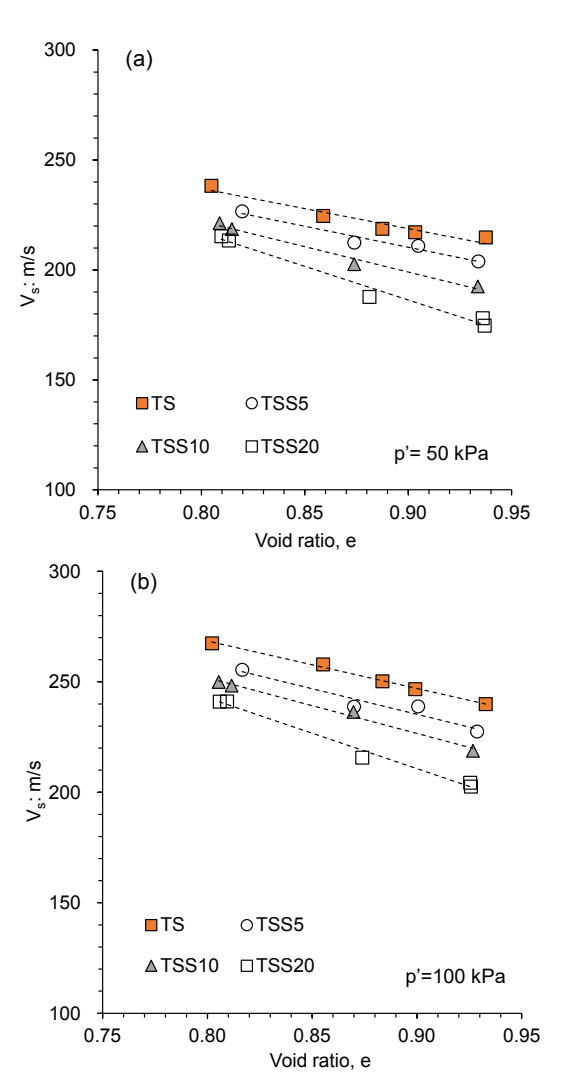


Fig. 10. Shear wave velocity versus void ratio at two stress levels (data from Yang and Liu 2016)

By introducing a stress-corrected shear wave velocity  $(V_{sI})$ , a linear relationship between  $V_{sI}$  and e can readily be established as:

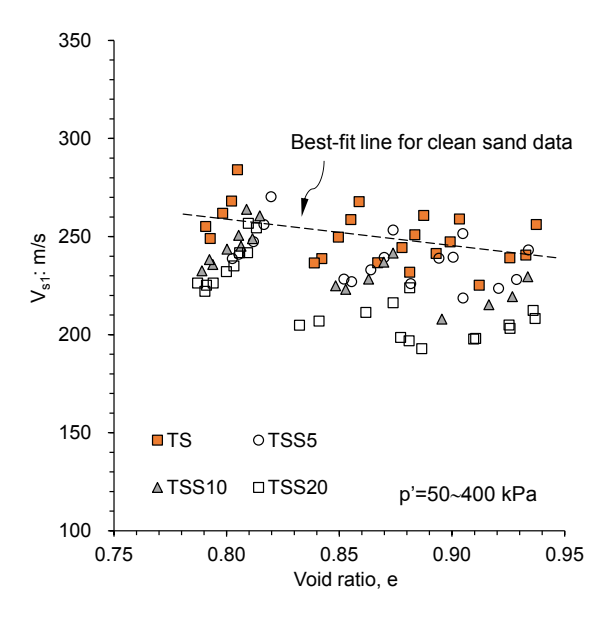


Fig. 11. Stress-corrected shear wave velocity versus void ratio

$$V_{s1} = V_s \left(\frac{p_a}{p'}\right)^{1/4} = (b_1 - b_2 e)$$
 (3)

The above relationship is commonly used in geotechnical engineering practice. When all measured  $V_s$  values are corrected for stress and then plotted against void ratio, as given in Fig. 11, one can see that this linear relationship fails to work in an acceptable way.

# 4.2 State parameter-based characterization of shear wave velocity

All shear wave tests were conducted on saturated specimens and covered a wide range of states in terms of void ratio and effective confining stress (Yang and Liu 2016). To determine the state parameters of these specimens, the critical state lines of the tested materials in the compression space are required. Fig. 12 show the critical state loci of TS, TSS5, TSS10 and TSS20 in the e- $(p'/p_a)^\xi$  space, here  $\xi$  takes a typical value of 0.6 (Yang and Li 2004). Note that the critical state locus moves downward with increasing fines content. By calculating the state parameters, the measured  $V_s$  values for clean and mixed sand specimens (TS, TSS5, TSS10, TSS20) can be presented as a function of  $\psi$ , as shown in Fig. 13 for two stress levels (50 kPa and 100 kPa) as an example.

A striking finding is that for either stress level, all data points fall on a single straight line, regardless of fines content. This finding is significantly different from the observation in Fig. 10, obtained from the traditional method of analysis. Furthermore, using the concept of stress-corrected shear wave velocity, a unique relationship can be established between  $V_{\rm s1}$  and  $\psi$ , which works surprisingly well for all data, as shown in Fig. 14. The relationship can be described using a simple, linear function:

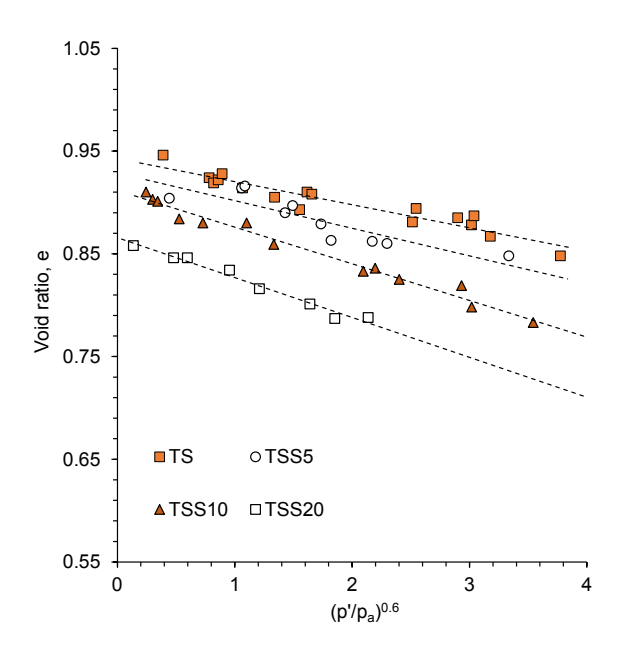


Fig. 12. Critical state loci of TS, TSS5, TSS10 and TSS20 (data from Yang and Wei 2012)

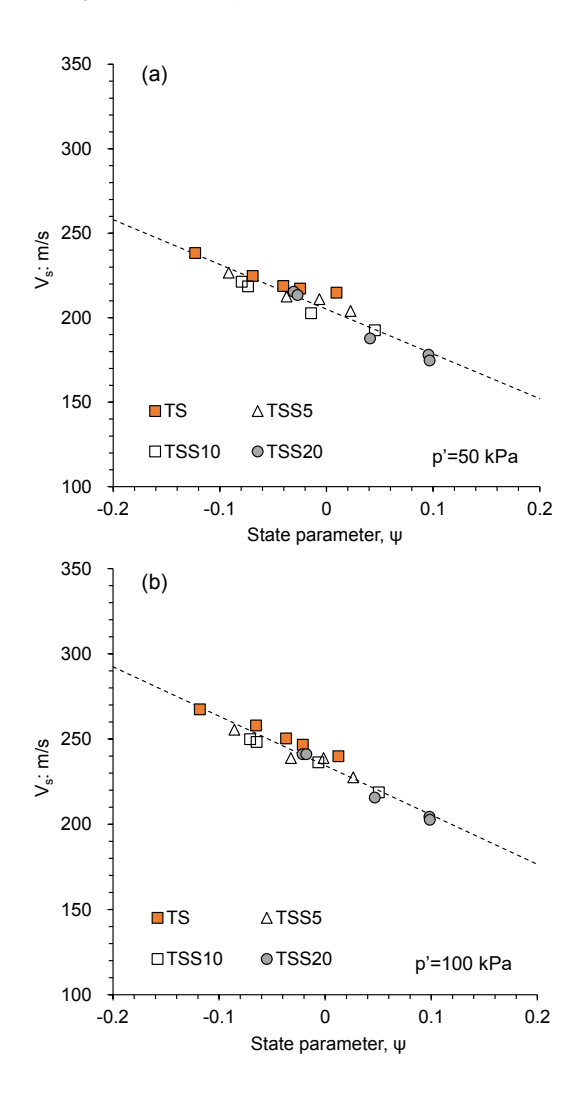


Fig. 13. Shear wave velocity versus state parameter at two stress levels.

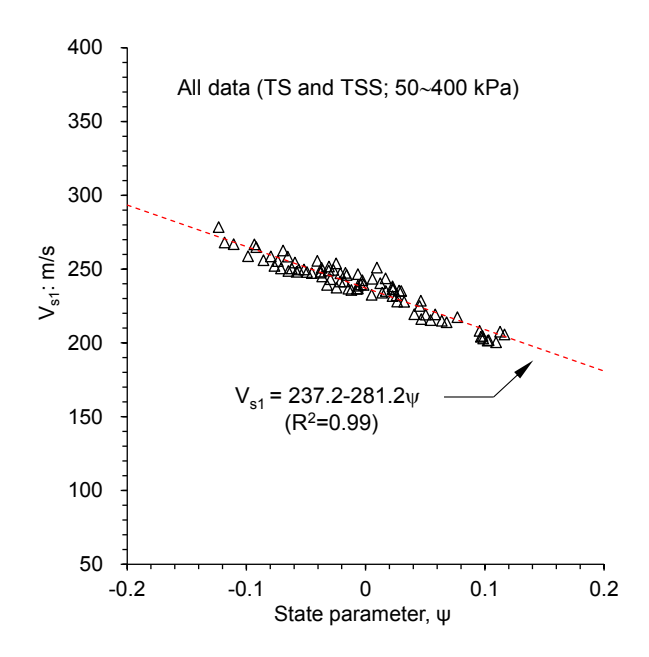


Fig. 14. Stress-corrected shear wave velocity versus state parameter for TSS series data (after Yang et al. 2018)

$$V_{s1} = V_s \left(\frac{p_a}{p'}\right)^n = A - B\psi \tag{4}$$

where A, B and n are material constants dependent on particle characteristics. From the test results they are determined as 237.2 m/s, 281.2 m/s, and 0.222, respectively. For other quartz sands and fines which share similar grain characteristics as the materials tested in this study, these values are likely to remain at similar levels. Also, it is found that if a default value of 0.25 is assigned to n, the performance of the above relationship remains reasonably good although the degree of scatter becomes a bit larger (Yang et al. 2018).

#### 5 EVALUATION OF IN-SITU STATE OF SAND

Freshly deposited sands are generally under normally consolidated, anisotropic conditions. The mean effective stress p' at a given depth can be estimated as

$$p' = \left(\frac{1 + 2K_0}{3}\right)\sigma_{\nu}' \tag{5}$$

where  $\sigma_v$ ' is effective vertical stress at the depth and  $K_0$  is the coefficient of earth pressure at rest. Combining Eq. (5) with Eq. (4) gives rise to an alternative form for state-dependent  $V_s$  as follows

$$V_s = (A - B\psi) \left(\frac{\sigma_v'}{p_a}\right)^n \left(\frac{1 + 2K_0}{3}\right)^n \tag{6}$$

Note that values of  $K_0$  for normally consolidated, loose and medium dense sands typically vary between 0.4 and 0.6.

Using the above relationship and the parameters for the sand-fines mixtures tested, Fig. 15 shows the curve for the specific state parameter ( $\psi = 0$ ) for an assumed  $K_0$  value (0.5). The curve approximately defines the boundary between a dilative-response zone and a contractive-response zone. If the sand state lies in the contractive zone, caution should be exercised that the sand has a potential for liquefaction when subjected to undrained shear. A more comprehensive view of the state profiles is given in Fig. 16, where a set of curves, representing states varying from  $\psi = -0.2$  (highly dilative) to  $\psi = +0.2$  (highly contractive and liquefiable), is included.

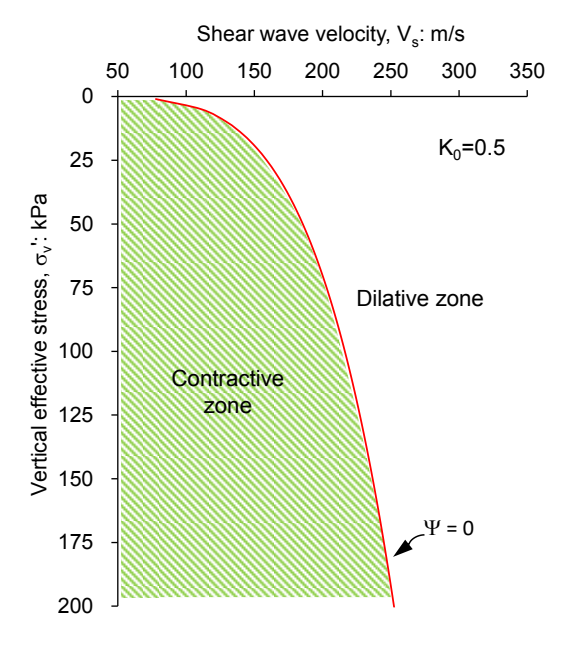


Fig. 15. State boundary of TSS series in the  $V_s$ - $\sigma_v$ ' plane at  $K_0$  =0.5

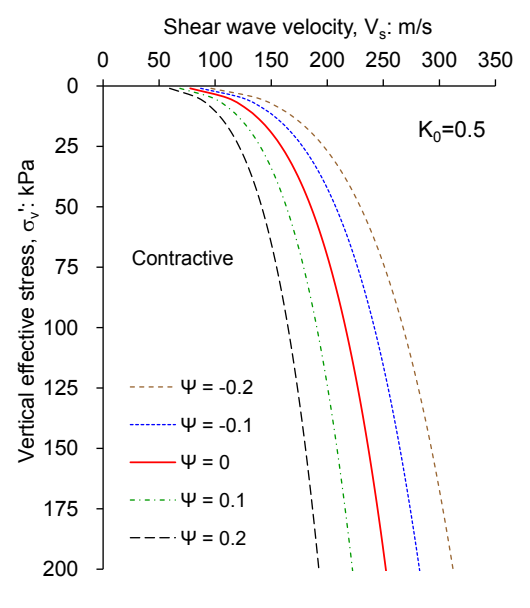


Fig. 16. State profiles of TSS series in the  $V_s$ - $\sigma_v$ ' plane at  $K_0 = 0.5$ 

### 6 VALIDATION USING INDEPENDENT TEST DATA

The significance of Eqs. (4) and (6) is that they provide a unified relationship linking  $V_s$  and  $\psi$  for both clean and silty sands. To validate this relationship, two independent specimens were prepared: one composed of clean Toyoura sand only (TS) and the other composed of 90% Toyoura sand and 10% fines (TSS10). The TS specimen was isotropically consolidated to the state of e=0.846 and p'=100 kPa, whereas the TSS10 specimen was consolidated to the state of e=0.904, p'=300 kPa. For both specimens, their shear wave velocities were measured using the piezoelectric bender elements. Fig. 17 shows received signals at the excitation frequency of 10 kHz, giving the  $V_s$  values of 257.5 m/s (TS) and 281.2 m/s (TSS10), respectively. By direct comparison of the measurements, one may arrive at the conclusion that the TSS specimen with higher  $V_s$  is at a denser state and hence is less susceptible to liquefaction. However, this conclusion can be misleading.

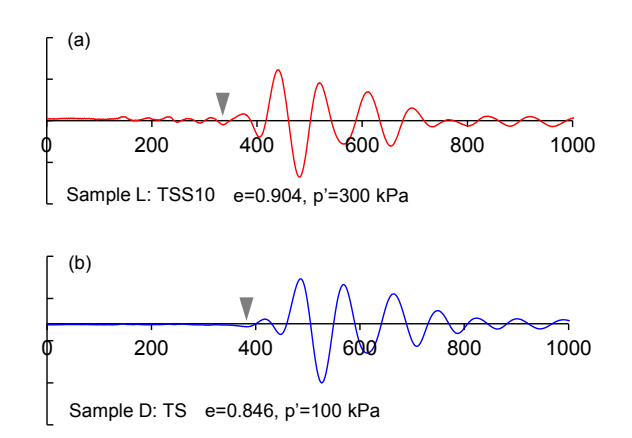


Fig. 17. Shear wave signals in two independent specimens at excitation frequency of 10 kHz

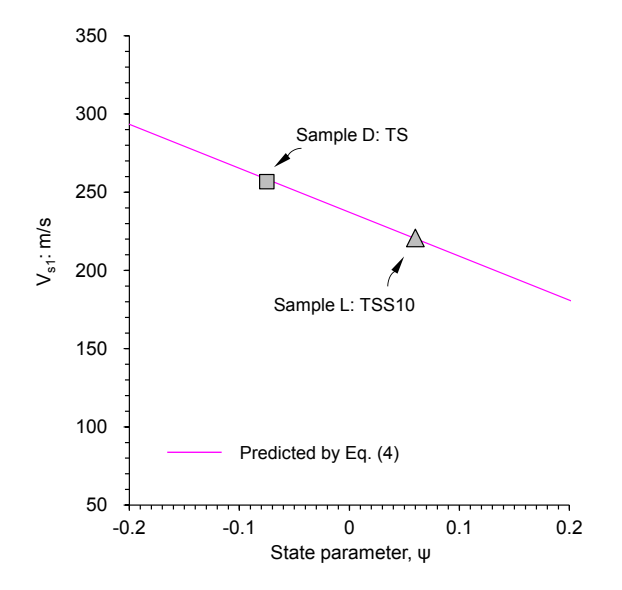


Fig. 18. Stress-corrected shear wave velocity versus state parameter: prediction versus measurement

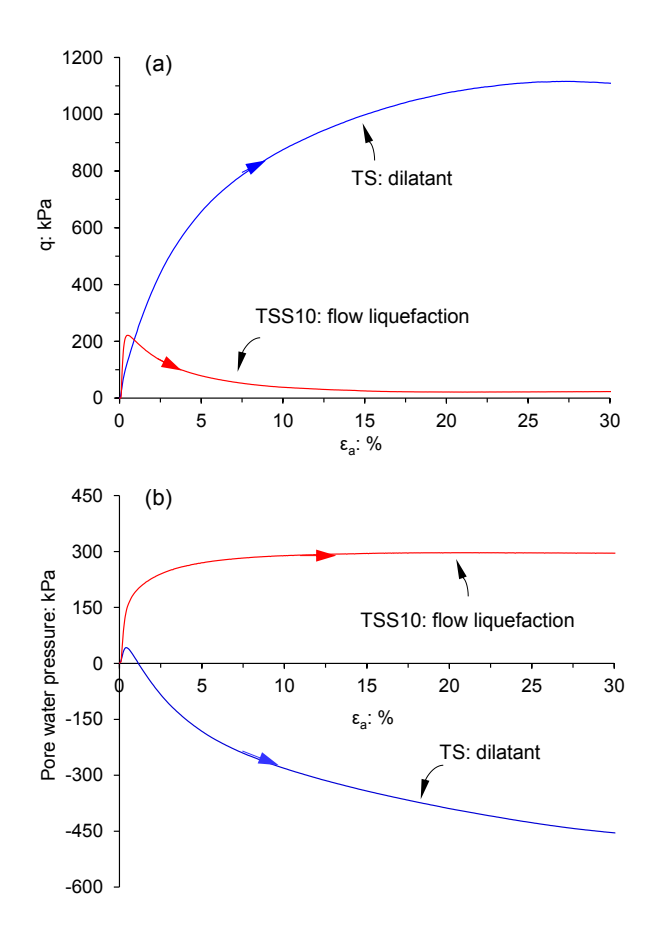


Fig. 19. Undrained shear responses of two independent specimens.

A more rational comparison can be made in the  $V_{\rm s1}$  -  $\psi$  plane as shown in Fig. 18, which shows that the TSS10 specimen with higher  $V_{\rm s}$  is actually at a *looser* state ( $\psi$  = +0.060) whereas the TS specimen with lower  $V_{\rm s}$  is at a *denser* state ( $\psi$  = -0.075). Note that the solid line on the plot is the prediction made using Eq. (4) while the two data points are obtained from independent tests. The agreement between prediction and measurement is markedly high.

In line with the concepts of state parameter shown in Fig. 3 and Fig. 15 and given the state parameters determined, one may predict that the TSS10 specimen under undrained shear tends to exhibit a contractive, liquefiable behavior whereas the TS specimen tends to exhibit a dilative, non-liquefiable response. To verify the prediction, undrained monotonic triaxial tests were conducted on the two specimens. The results in terms of the stress-strain curve and pore water pressure generation are shown in Fig. 19. Strikingly, the TSS specimen, as predicted, underwent almost complete liquefaction, with an extremely low strength at the critical state, whereas the TS specimen exhibited a highly dilative response, with a large strength attained at the critical state.

Given the significance of the correlation between the shear wave velocity and the state parameter, further validation using literature data is desirable. However, there is a lack of studies that contain adequate information for interpretation in this respect in literature. Huang et al. (2004) reported test data on shear wave velocity ( $V_s$ ) for a natural silty sand with different quantities of fines, measured at a confining pressure of 100 kPa using bender elements installed in a triaxial device. They also conducted monotonic loading tests leading to the information on critical states, but the test data were analyzed using the conventional method of Hardin and Richart (1963).

Re-interpretation of these data is shown in Fig. 20. When the measured shear wave velocity is plotted against void ratio, different trend lines exist for different fines contents (Fig. 20a). For a given void ratio, the effect of fines is a decrease of shear wave velocity, being consistent with the finding in Fig. 10. By calculating the state parameter for the tested samples and then plotting the shear wave velocity as a function of the state parameter, a unique trend line fitting all data points can be drawn (Fig. 20b), regardless of fines content. This finding demonstrates that the relationship in Eq. (4) also works well for the natural silty sand.

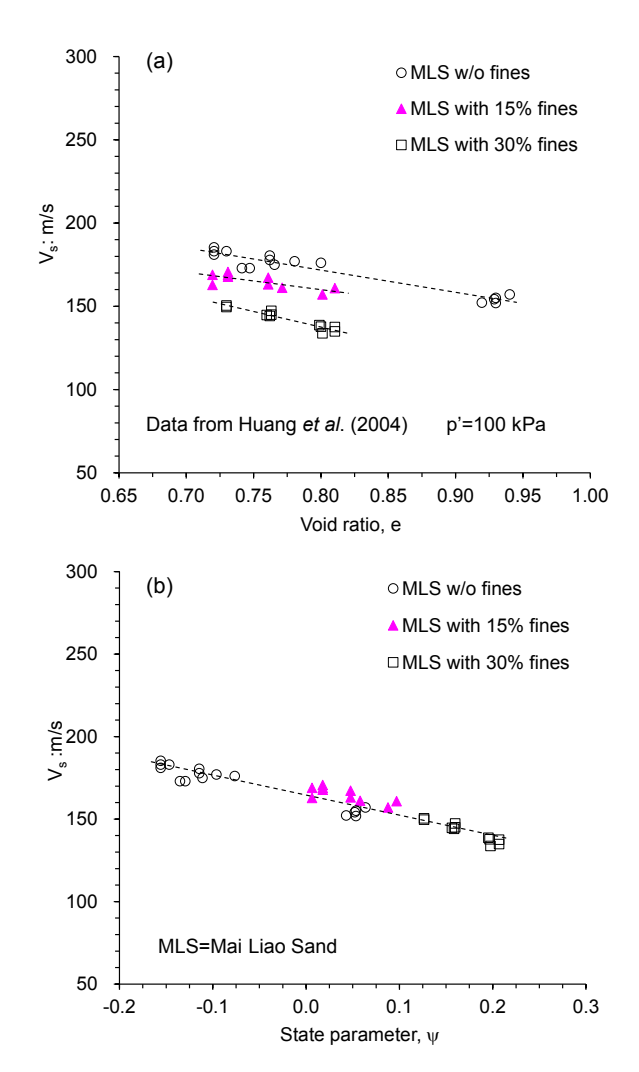


Fig. 20. Re-interpretation of experimental data on a natural silty sand

# 7 RELATIONSHIP BETWEEN SHEAR WAVE VELOCITY AND CYCLIC RESISATNCE

A systematic experimental program on cyclic behavior and liquefaction resistance of sand-fines mixtures has also been carried out to examine whether the correlation between cyclic resistance ratio and state parameter, established based on experimental data on clean sands (Eq. (1)), work for different sand-fines mixtures (Wei and Yang 2019a, 2019b, 2023). Selected results are shown in Fig. 21. Strikingly, all data points for the sand-fines mixtures fall into the vicinity of the best-fit line for clean Toyoura sand, suggesting that there exists a *unified* CRR-ψ correlation for these sand-fines mixtures. If CRR is determined using a different number of cycles to failure (e.g., 15 or 20), the relationship taking the form in Eq. (1) is expected to work as well.

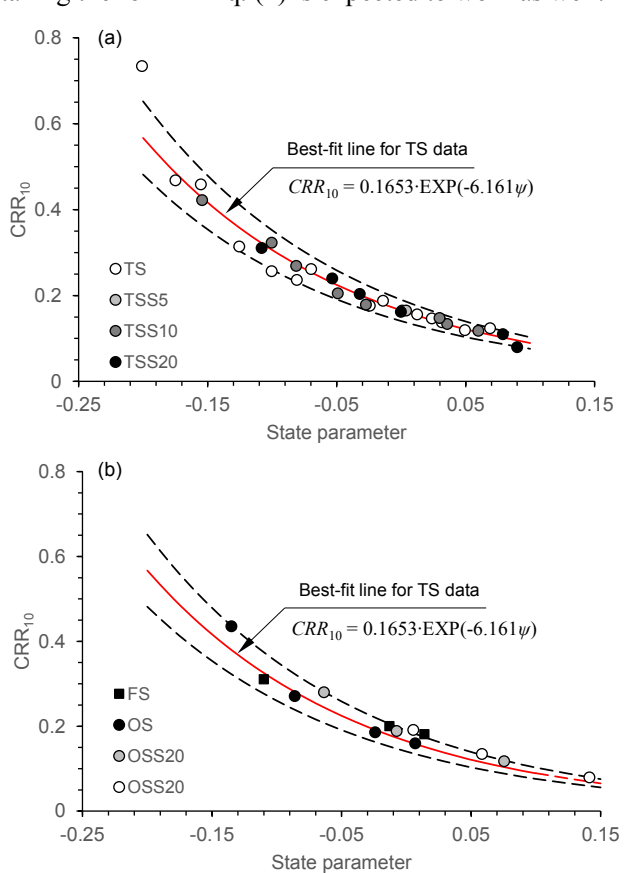


Fig. 21. Unified CRR- $\psi$  relationship for different sand-fines mixtures (data from Yang and Sze 2011; Wei and Yang 2023)

With the validated relationships in Eq. (1) and in Eq. (4), a new relationship linking the cyclic resistance ratio and shear wave velocity can be derived:

$$CRR_{10} = a \cdot \exp\left[-\frac{b}{R} \cdot (A - V_{s1})\right] \tag{7}$$

The novelty of this relationship lies in that it is built on systematic experimental datasets comprising both smallstrain shear wave testing and large-strain cyclic shear testing and covering a range of states and fines contents and it is formulated in a solid theoretical context. In this regard, it is significantly different from the empirical  $V_{\rm s}$ -based liquefaction charts in current engineering practice, which were developed using case history data from past earthquakes and thus contained considerable uncertainties. Due to the empirical nature, these charts do not properly incorporate the physics involved. One of the marked features of the new relationship in Eq. (7) is that, for a given base sand and its mixtures with fines, the relationship is independent of fines content. Detailed discussion on its applications and the comparisons with existing empirical charts will be presented in future.

#### 8 MICROMECHANICAL MECHANISMS

Keeping in mind the granular nature of sandy soils, it is of interest to explore the micro-scale mechanism for the observed effects of fines on the shear wave velocity as well as on the liquefaction resistance of sand. In the context of micromechanics, the coordination number is a simple yet key index describing the arrangement of discrete particles in an assembly under a given confinement; it is defined as the average contact number per particle. Drawing on this grain-scale consideration, it is hypothesized that the reduction of shear wave velocity or shear stiffness caused by the presence of fines is mainly associated with the reduction in the coordination number. This hypothesis is schematically shown in Fig. 22.

Three idealized packings represent three cases: Case (a) is for clean sand without fines, Case (b) is for sand with a small quantity of fines, and Case (c) for sand with a relatively large quantity of fines. Note that all three packings have the same solid fraction and hence the same void ratio, but they possess different coordination numbers. For the clean sand case, the coordination number is the highest and hence its shear stiffness is the largest, whereas in Case (c) the coordination number is the least and correspondingly its shear stiffness is the smallest. This hypothesis has been verified by 3D DEM simulations of random assemblies of spherical particles of coarse and fine sizes under triaxial loading (Fig. 23); more interesting results in this regard can be found in Luo and Yang (2013) and Dai et al. (2015).

Furthermore, the discrete element simulations of wave propagation in granular materials (Tang and Yang 2020) have revealed that the presence of fines does not only change the wave velocity, but also the frequency transmission. Even a small quantity of fines is mixed in, the frequency filtering and attenuation effects can become rather prominent, see Fig. 24.

Other grain-scale properties that may cause notable effects on the shear wave velocity and shear resistance of sand include particle shape and size disparity ratio (Figs. 25 and 26). The relevant experimental results and numerical simulations can be found in Wei and Yang (2014), Yang and Luo (2015), Liu and Yang (2018), Tang and Yang (2021) and Wei and Yang (2023).

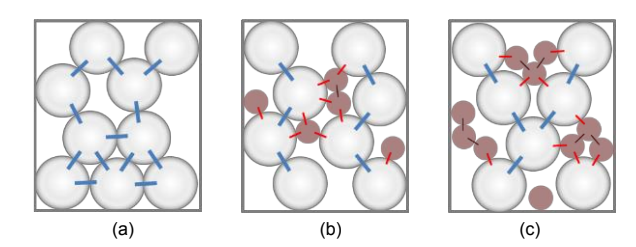


Fig. 22. Micro-mechanism for fines effect on shear wave velocity and liquefaction potential (after Yang and Liu 2016)

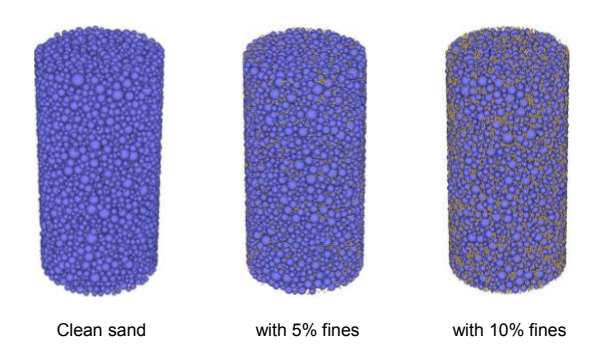


Fig. 23. Specimens of clean sand and sand-fines mixtures in discrete element simulations (after Luo and Yang 2013)

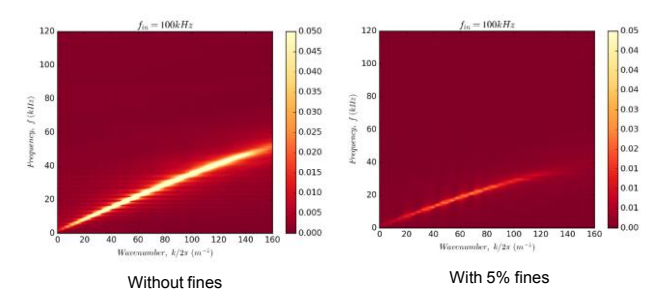


Fig. 24. Effects of fines on dispersion relationship (after Tang and Yang 2020)  $\,$ 

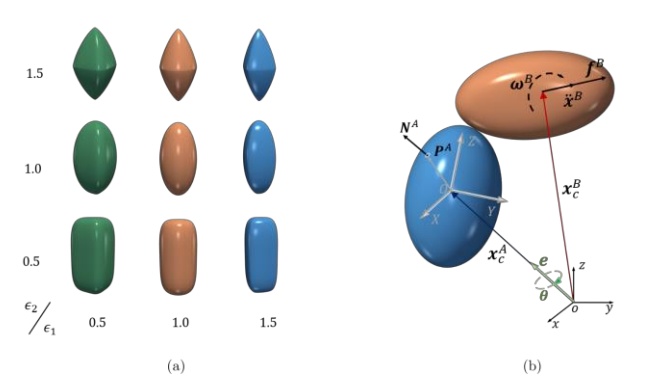


Fig. 25. Use of superquadric particles in discrete element simulations of particle shape effect (after Tang and Yang 2021)

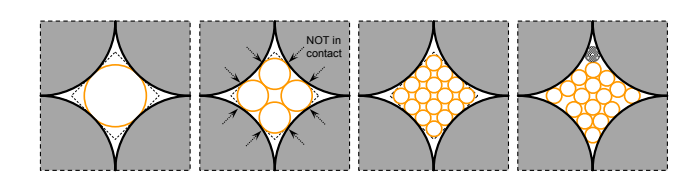


Fig. 26. Schematic illustration of grain-scale mechanism for size disparity effect (after Wei and Yang 2023)

#### 9 CONCLUDING REMARKS

Properly estimating the in-situ state of sand deposits with fines and their potential for liquefaction is a challenging problem in geotechnical engineering. This paper presents a new and promising method for this purpose. The significant advantage of the method is that it accounts for the complex effects of fines in a unified manner in the context of the critical state theory. Central to the method is a unique relationship established between  $V_{\rm s1}$  and  $\psi$  that is independent of fines content. Compared with the cone penetration resistance widely used in current geotechnical applications, shear wave velocity is a basic soil property with clear physical meaning, and can be measured in soils that are hard to penetrate with the penetrometer or at sites where borings may not be permitted. Modern technology has advanced such that shear wave velocity can be measured more conveniently and reliably both in the laboratory (e.g., piezoelectric bender elements) and in the field (e.g., SASW and seismic CPT). Compared with the relative density  $D_{\rm r}$ , the state parameter  $\psi$  is a more rational state variable for characterizing various aspects of soil behavior under both cyclic and monotonic loading conditions. All these advantages make the new method appealing to a variety of geotechnical applications.

Further studies to refine the method based on laboratory and field tests on different sands with different grain characteristics are much needed and worthwhile. Also, it is necessary to acknowledge that the method is mainly applicable to fresh, unaged sand deposits or fills. To what extent it is applicable to aged or cemented sand deposits is yet unclear; future research to explore this issue in the proposed framework would be of interest. Nevertheless, it is important to bear in mind that it is the fresh, unaged sand deposits that are susceptible to liquefaction and excessive deformation.

### **ACKNOWLEGEMENTS**

The work presented in this keynote lecture is part of long-term research on soil liquefaction and related phenomena from the multi-scale perspectives, conducted at the University of Hong Kong (HKU). The author is grateful for the financial support provided by the Research Grants Council of Hong Kong over the years (Nos. C7038-20G, 17206119, 17206418, 17250316, 719105). The author also wishes to thank the postgraduate students who worked with him on these projects. The invitation of the organizing committee of the 8<sup>th</sup> International Conference on Earthquake Geotechnical Engineering to deliver this keynote lecture is highly appreciated.

#### REFERENCES

 Baldi, G., Bellotti, R., Chionna, V., Jamiolkowski, M., Pasqualini, E. (1982): Design parameters for sands from CPT,

- In Proceedings of 2nd European Sym. on Penetration Testing, Amsterdam, Holland, 425-432.
- 2) Been, K., Jefferies, M.G. (1985): A state parameter for sands, *Géotechnique*, 35(2), 99–102.
- 3) Been, K., Crooks, J.H. A., Becker, D.E., Jefferies, M.G. (1986): The cone penetration test in sands. Part 1: State parameter interpretation, *Géotechnique*, 36(2), 239-249.
- Casagrande, A. (1975): Liquefaction and cyclic deformation of sands, a critical review. In *Proceedings of 5th Pan-American Conference on Soil Mech. Found. Eng., Buenos Aires*, 5, 79–133.
- Castro, G. (1975): Liquefaction and cyclic mobility of saturated sands, *J. Geotech. Eng. Division*, ASCE, 101(GT6), 551-569
- Clayton, C.R.I. (2011): Stiffness at small-strain: research and practice, Géotechnique, 61(1), 5–38.
- Dai, B., Yang, J., Luo, X.D. (2015): A numerical analysis of the shear behavior of granular soil with fines, *Particuology*, 21, 160-17.
- Gu, X.Q., Yang, J., Huang, M.S., Gao, G.Y. (2015): Bender element tests in dry and saturated sand: Signal interpretation and result comparison, *Soils Founds*, 55(5), 951-962.
- Hardin, B.O., Richart, F.E. (1963): Elastic wave velocities in granular soils, *J. Soil Mech. Found. Div.*, ASCE, 89(SM1), 39–56.
- Huang, Y.T., Huang, A.B., Kuo, Y.C., Tsai, M.D. (2004): A laboratory study on the undrained strength of a silty sand from Central Western Taiwan, *Soil Dynamics Earthquake Eng.*, 24, 733-743.
- 11) Idriss, I.M., Boulanger, R.W. (2006): Soil liquefaction during earthquakes, EERI Monograph.
- 12) Ishihara, K. (1993): Liquefaction and flow failure during earthquakes. *Géotechnique*, 43(3), 351-451.
- 13) Jamiolkowski, M. (2014): Soil mechanics and the observational method: challenges at the Zelazny Most copper tailings disposal facility, *Géotechnique*, 64(8), 590-619.
- 14) Liu, X., Yang, J. (2018): Shear wave velocity in sand: effect of grain shape, *Géotechnique*, 68(8), 742-748.
- 15) Lunne, T., Robertson, P.K., Powell, J.J.M. (1997): Cone penetration testing in geotechnical practice, Blackie Academic & Professional (Chapman & Hall), Glasgow, U.K.
- 16) Luo, X.D., Yang, J. (2013): Effects of fines on shear behavior of sand: a DEM analysis, In *Proceedings of 5th Int. Young Geotech. Engineers' Conference*, Paris, France, IOS Press, 265–268.
- 17) Mayne, P.W. (2007): Cone penetration testing, NCHRP Synthesis 368, Transportation Research Board, Washington, D.C.
- 18) Murthy, T.G., Loukidis, D., Carraro, J., Prezzi, M., Salgado, R. (2007): Undrained monotonic response of clean and silty sands. *Géotechnique*, 57(3), 273-288.
- Polito, C.P., Martin, J.R. (2001): Effects of nonplastic fines on the liquefaction resistance of sands, *J. Gotech. Geoenviron.* Eng., ASCE, 127(5), 408-415.
- Robertson, P.K., Sasitharan, S., Cunning, J.C., Sego, D.C. (1995): Shear wave velocity to evaluate flow liquefaction, *J. Geotech. Eng.*, ASCE, 121(3), 262-273.
- 21) Seed, H.B. (1979): Soil liquefaction and cyclic mobility evaluation for level ground during earthquakes, *J. Geotech. Eng. Div.*, ASCE, 105(2), 201-255.
- Seed, H.B., Lee, K.L. (1996): Liquefaction of saturated sands during cyclic loading, *J. Soil Mech. Founds. Div.*, ASCE, 92 (SM6), 105-134.
- 23) Stokoe, K.H. (2007): Field seismic testing in geotechnical earthquake engineering, In *Proceedings of 4th Int. Conference on Earthquake Geotechnical Engineering*, 151-157.

- 24) Sze, H.Y., Yang, J. (2014): Failure modes of sand in undrained cyclic loading: Impact of sample preparation, *J. Geotech. Geoenviron. Eng.*, ASCE, 140(1), 152-169.
- 25) Tang, X., Yang, J. (2020): Wave propagation in granular material: effects of fines. *Technical Report*, Department of Civil Engineering, The University of Hong Kong.
- 26) Tang, X., Yang, J. (2021): Wave propagation in granular material: What is the role of particle shape? *J. Mech. Physics Solids*, 157, 104605.
- 27) Thevanayagam, S., Fiorillo, M., Liang, J. (2000): Effect of non-plastic fines on undrained cyclic strength of silty sands. In Soil Dynamics and Liquefaction, ASCE.
- 28) Vaid, Y.P., Stedman, J.D., Sivathayalan, S. (2001): Confining stress and static shear effects in cyclic liquefaction, *Can. Geotech. J.*, 38(3), 580-591.
- 29) Wang, W.S. (1981): Liquefaction mechanism of soil, *Chinese J. Hydraulic Eng.*, 5, 22-34.
- 30) Wei, L.M., Yang, J. (2014): On the role of grain shape in static liquefaction of sand-fines mixtures, *Géotechnique*, 64(9), 740-745.
- Wei, X., Yang, J. (2019a): Cyclic behavior and liquefaction resistance of silty sands with presence of initial static shear stress, Soil Dynamics Earthquake Eng., 122, 274-289.
- 32) Wei, X., Yang, J. (2019b): Characterizing the effects of fines on the liquefaction resistance of silty sands, *Soils Founds*, 59(6), 1800-1812.
- 33) Wei, X., Yang, J. (2023): Characterising the effect of particle size disparity on liquefaction resistance of non-plastic silty sands from a critical state perspective, *Géotechnique*, 73(4), 323-336.
- 34) Wichtmann, T., Hernandez, M., Triantafylidis, T. (2015): On the influence of a non-cohesive fines content on small strain stiffness, modulus degradation and damping of quartz sand, *Soil Dynamics Earthquake Eng.*, 69, 103–114.
- 35) Yamamuro, J.A., Lade, P.V. (1997): Static liquefaction of very loose sands, *Can. Geotech. J.*, 34(6), 905–917.
- 36) Yang, J. (2002): Non-uniqueness of flow liquefaction line for loose sand, *Géotechnique*, 52(10), 757–760.
- 37) Yang, J., Gu, X.Q. (2013): Shear stiffness of granular material at small strains: does it depend on grain size? *Géotechnique*, 63(2), 165-179.
- 38) Yang, J., Li, X.S. (2004): State-dependent strength of sands from the perspective of unified modeling, *J. Geotech. Geoenviron. Eng.*, ASCE, 130(2), 186–198.
- 39) Yang, J., Liang, L., Chen, Y. (2022): Instability and liquefaction flow slide of granular soils: the role of initial shear stress, *Acta Geotechnica*, 17, 65-79.
- 40) Yang, J., Liu, X. (2016): Shear wave velocity and stiffness of sand: the role of non-plastic fines, *Géotechnique*, 66(6), 500-514.
- 41) Yang, J., Liu, X., Guo, Y., Liang, L.B. (2018): A unified framework for evaluating in-situ state of sand, *Géotechnique*, 68(2), 177-183.
- Yang, J., Luo, X.D. (2015): Exploring the relationship between critical state and particle shape for granular materials, J. Mech. Physics Solids, 84, 196-213
- 43) Yang, J., Sze, H.Y. (2011a): Cyclic behaviour and resistance of saturated sand under non-symmetrical loading conditions, *Géotechnique*. 61(1), 59-73.
- 44) Yang, J., Sze, H.Y. (2011b): Cyclic strength of sand under sustained shear stress, *J. Gotech. Geoenviron. Eng.*, ASCE 137(12), 1275-1285.
- 45) Yang, J., Wei, L.M. (2012): Collapse of loose sand with the addition of fines: the role of particle shape, *Géotechnique*, 62(12), 1111–1125.

- 46) Yang, J., Wei, L.M., Dai, B.B. (2015): State variables for silty sands: global void ratio or skeleton void ratio? *Soils Founds*, 55(1), 99-111.
- 47) Youd, T.L., Idriss, I.M., Andrus, R.D., Castro, G., Christian, J.T., Dobry, R., Finn, W.D.L., Harder, L.F., Jr., Hynes, M.E., Ishihara, K., Koester, J.P., Liao, S.S.C., Marcuson III, W.F., Martin, G.R., Mitchell, J.K., Moriwaki, Y., Power, M.S., Robertson, P.K., Seed, R.B., Stokoe II, K.H. (2001): Liquefaction resistance of soils: summary report from the 1996 NCEER and 1998 NCEER/NSF workshops on evaluation of liquefaction resistance of soils, *J. Geotech. Geoenviron. Eng.*, ASCE, 127(10), 817-833.